

Extraction of Tactile Features by Passive and Active Sensing

R. E. Ellis

COINS Technical Report 84-27

**Laboratory for Perceptual Robotics
Department of Computer and Information Science
University of Massachusetts
Amherst MA 01003**

ABSTRACT

Tactile sensors which are mounted on a robot gripper are typically much smaller than the objects they touch. If the robot system is to use a tactile sensor to perform such tasks as object recognition, parts inspection, or manipulation, then integration of features extracted from multiple sensing incidents will be necessary.

This paper describes ways of acquiring tactile features that may be used in such tasks. Extraction of such features requires knowledge of the inherent advantages and limitations of tactile array sensors, and how the information they provide can be combined with information from position and force sensors. A number of tactile features (such as edge radii and object deformation) are best acquired by active sensing, in which the sensor is moved with respect to the object in a known fashion. Some strategies for extraction of tactile features, in both passive and active sensing paradigms, are presented and discussed.

50 Introduction

Tactile features are those that can be sensed by direct contact between a set of sensors and objects in the environment. Having assumed that a sensor is mounted on a robot, the direct contact sensing discussed below will focus on *haptic sensing*. The haptic senses are defined, for the robot domain, in a manner similar to the biological: they include information on the position, orientation, velocity, and forces sensed by the joints and limbs, and the data provided by tactile array sensors (hereafter, TA's).

Because of the high density, good quality, and regular geometry of tactile images available from many current planar TA's, it is often tempting to think of them as "little touch pictures" of the object being sensed. This approach may be appropriate when the object's size is less than, or approximately the same size as, that of the sensor, or when a complex set of features is expected to occur in a single tactile image. However, in the more typical case where the sensor is much smaller than the object or the object presents only simple features, performing complex visual-like analysis of tactile images seems inappropriate.

When the task is object recognition, inspection, or manipulation, various features of the object are needed to identify it as matching a known model (or, if information is limited and errorful, as matching one of a few specifiable models). If one includes the proprioceptive senses available in a robot arm/hand, and assumes that the position, velocity and force applied to various joints and limbs are controllable, there are at least ten distinct tactile features that can be extracted. Some of these object features, such as line contact or point contact, can be gained by static (or passive) sensing; others, such as deformation and (to some degree) texture, require both multiple tactile sensing incidents with the same object *and* integration of these tactile data with those of other sensors. The features extracted, and the mode by which they are extracted, depend crucially upon the task and sensors available. The discussion below notes some important characteristics of tactile sensors, and in light of these considerations presents examples of tactile features extracted by passive and active sensing.

§1 Tactile Array Sensors

There has been considerable interest recently in the production and use of tactile array sensors for robotics applications. Detailed discussion of such sensors may be found in. e.g. [Allen, 1983], [Begej, 1984], [Boie, 1984], [Briot, 1979], [Clot & Falipou, 1979], [Hillis, 1981], [Rebman & Trull, 1983], [Overton, 1984], [Raibert & Tanner, 1982], and [Wright, 1983]. Note that of these, only the Allen work is with a non-planar sensor. Consequently, although non-planar sensors can be constructed and have interesting properties of their own, the following discussion will assume that the TA is planar and regular in geometry (i.e. has a square, rectangular, triangular, or other simple layout of its sensing elements).

All of these sensors operate, ultimately, by sampling the distribution of strains over the sensor surface. If we disregard the first version of the Rebman sensor, which had a knobby surface, this statement can be strengthened to saying:

Modern tactile array sensors sample the distribution of strains in a homogeneous [planar] medium.

The density of the sampling varies considerably. One may roughly distinguish among various sensors by looking at the order of magnitude of the number of strain samples taken per cm^2 . Thus a low density tactile array (LDTA) has about 1 tactile element, or *taxel*, per cm^2 ; a medium density tactile array (MDTA) has about 10 per cm^2 ; a high density tactile array (HDTA) has about 100 per cm^2 ; and a very high density tactile array (VHDTA) has on the order of 1000 per cm^2 .

Other factors that are important in assessing a TA are: the working range of each taxel; the resolution (i.e. number of distinct, reliable output levels over the working range) of a taxel; the net size of the sensing area, as opposed to the number of taxels in that area; the degree to which the sensor responds to shear v. normal forces; and the compliance of the sensor pad and backing to various stress distributions.

In assessing the usefulness of a given sensor for a particular task, it should be remembered that the task of the sensor is to distinguish object features with some minimal acceptable reliability. For some applications, binary (two-valued) taxels may be

quite sufficient, whereas for fine manipulation many bits of information per taxel may be required. Similarly, some tasks may require a high density but only really call for it over a small area, whereas other tasks, such as detecting collisions of a limb with objects, do not need many taxels but needs them with very few "dead" zones.

The sensors used in our lab are HDTA's and VHDTA's, with the active sensing area 6-11 cm² in size. The taxel geometries are rectangular, square, and triangular, and all can have a pad compliance approximately equivalent to that of a researcher's fingertip. Sensitivity is from 5 to 8 bits over a working pressure of 60 psi (as applied hydrostatically over the entire active area of the sensor).

§2 Analysing Tactile Array Data

As stated above, the primary analysis of tactile data is in the extraction of features. Some of the features that may be extracted by our laboratory's sensing system are:

- Three-dimensional position of the area of contact of the sensor and object, relative to the robot's base reference frame.
- A measure of the planarity of the contact area.
- If the contact is with a plane, the surface normal of that plane.
- Whether the the area of contact seems to be an edge, rather than a gently-curved surface.
- Whether the contact is with a corner or vertex, rather than an edge or surface.
- Whether there are slots present in the area being sensed.
- Whether there are holes present in the surface or edge being sensed.
- A measure of the surface texture of the area of contact.
- An estimate of the radius of curvature of an edge or corner.
- The manner in which the object deforms in application to a force (assuming it is somehow firmly supported).

Feature extraction can be *passive*, i.e. features can be found from a single tactile sensor which is brought into contact with an object, or *active*, i.e. feature extraction requires that the sensor be moved with respect to the object. In the above list, the last two definitely require active touch sensing; texture, while it can be measured passively, probably is better measured actively.

The results below show examples of extraction of various features by our system. It is implemented on a VAX 11/750 in a combination of LISP and FORTRAN. All of the tactile data presented here are taken with a VHDTA that is 3.3 cm on a side, arranged in a 128×128 square array (approximately 1504 taxels/cm²); the sensor is described in [Begej, 1984].

§2.1 Passive Touch Sensing

Static features that can be extracted include: whether the contact is with a corner, edge, or surface; whether there are any notable impressions on or depressions in the edge or surface; a measure of the texture of the contact; and where the TA the feature is located. The first six can be found using standard computer vision algorithms, and the last is just noting the location of the feature on the TA. (Since position of the array is known relative to the robot reference frame, the position and orientation of the feature can be located absolutely.)

Figure 1 shows the digitised image of a ball point pen tip pressed against the surface of a 8 bit/taxel VHDTA. Figure 3A shows edge contact with a linear object, and figure 4A contact with an arcing edge (the top of a soft drink can). These images were processed by passing an edge operator over them to extract prominent changes in intensity. The edge operator is the one proposed in [Canny, 1983], and is designed to detect and locate step edges in the presence of white noise.

Figures 3B and 4B show the edges found for the respective original images. An automated procedure attempted a least-squares fit of the data first to a line, and then to a circular arc. Point contact can be distinguished by the number of edges and the fact that both fits are poor; lines are distinguished from arcs by the RMS error of the fit. Plotting the fitted curves showed that the match of curve to data was very good, both mathematically and visually (spurious edges did not affect the procedure to any great degree).

Figure 5A shows an image of a washer, and figure 5B the edges extracted. The hole was located by assuming that contact should have been with a roughly circular, uniform object. Under this assumption, if the edge data are fit to a circle, then a hole is present if one or more diameters of the fit circle cross 4 edges: two for the circumference of the object, and two for the circumference of the hole. As can readily be seen, this algorithm extracts the presence of the hole.

The final passive sensing feature presented here are measures of texture. Figures 6, 7, and 8 show tactile images of a block of stiff conductive foam, the teeth of a wood rasp, and a piece of perforated steel screen. To human touch, these are of distinct and increasing texture.

Two texture measures were used. The first is the number of local maxima in the image, which correspond to the "high" points of the object; the other is the average height of these high points. To eliminate effects from noise and defects in the sensor (scratches on the glass plate), the images were smoothed with a Gaussian filter.

All three of the images were 128×128, with absolute pixel values ranging from 24 to 120. The texture measures (in units of pixels and image values), taken over the entire image, were:

Object	Maxima Count	Average Height
Foam	15	11.27
Screen	13	15.62
Rasp	31	15.19

The rankings assigned by these measures are in general agreement with human texture assessments. The rasp was highly textured, both in the number of points and in their intensity; the screen was much less textured, but presented the same "sharp" feelings of the rasp; and the foam, though notably textured, was much less intense than the other two samples. These results are just preliminary, and much work can be done on both passive and active measures of tactile texture.

§2.2 Active Touch Sensing

As stated above, one aspect of 'active touch sensing' involves movement of the sensor(s) relative to the object being touched. Analysis of the data involves processing multiple tactile images and/or integration of tactile and force information. Two such features are the radius of a contact edge, and determining the way an object deforms when pressed.

There are several ways of determining the edge radius; the one chosen was to simply press first with a light force and then with a heavy force on the edge, and note the differences in the tactile images. Figure 2A shows an edge of radius 3.2 mm pressed against the sensor with a force of 12 newtons; figure 3A shows the same edge pressed with a force of 39 newtons. The significant differences in the images are the

width of the edge, its mean intensity, and its average cross-section; all of these are greater in the second image.

The most sensitive (purely tactile) measure of deformation is the average cross-section. Due to non-linearities of the sensors we are now using in our laboratory, it is not feasible to calculate the radius. However, a good *estimate* of the edge radius for known applied forces can be found empirically. The method is to take some preferred application forces (which can be chosen to fit the task being performed), and press known edge radii against the sensor. Once such a table is constructed, selecting the best fit is a simple matter.

The cross-section analysis was performed by extracting the edges and fitting to a curve (in this case, the best fit was to a line). The cross-section was estimated by taking an average normal to the fitted curve; the width of the cross-section was determined by the mean width, as measured from the processed image. This average cross-section was then fit to an arc, and the deduced radius is the nearest in the empirical table.

The second active touch feature extracted was that of object deformation. Object deformation can be determined by pressing slightly, and then firmly, on an object. The force information, the change in position along the vector of force application, and the size and intensity of the tactile images can be integrated to determine roughly how the object behaves. Figures 9A and 10A show a racquet ball pressed against the sensor with normal forces of 12 newtons and 39 newtons respectively; figures 9B and 10B show the extracted edges. From the edge images the area consumed by the object may be estimated.

When the ball was pressed, it changed from its nominal diameter of 57 mm to 53 mm under 12 N. compression, and to 47 mm under 39 N. compression. The area changed from 674 pixels at 12 N. to 4681 pixels at 39 N. An acrylic sphere of 12.5 mm diameter, by comparison, showed no change in height under the same conditions, and a change in tactile area of 289 pixels to 487 pixels under the respective compressive forces. Clearly, it is possible to distinguish deformable objects from rigid objects on the basis of force combined with either positional information or, where this is not available, from tactile imprints.

§3 Conclusions

These results show the basic applicability of simple, computer vision inspired algorithms to the analysis of tactile data. Under the assumptions that multiple sensors are available, and that the tactile array sensor is much smaller than the sensed object, a number of tactile features can easily be extracted. These features are ones that can be expected to assist in recognition, manipulation, and inspection tasks, and thus have direct applicability to sensor-based robotics systems. Further investigation is being undertaken within the active sensing paradigm, and it is expected that this will lead to a better understanding of some problems in multi-sensory integration, and in the use of multiple senses to control robot motion.

Acknowledgements

The Laboratory for Perceptual Robotics is funded in part by NSF Grant ECS-8108818. Further support for this work was received from the National Sciences and Engineering Research Council of Canada.

I would like to thank Stefan Begej for developing the tactile sensor used in the experiments, and for his valuable comments on this paper.

Bibliography

- Allen, P. 1983. *Visually Driven Tactile Recognition and Acquisition*. Proceedings of the IEEE Conference on Computer Vision and Pattern Recognition, pp. 280-284.
- Begej, S. 1984. *An Optical Tactile Array Sensor*. Proceedings of the SPIE Conference on Intelligent Robots and Computer Vision.
- Boie, R.A. 1984. *Capacitive Impedance Readout Tactile Image Sensor*. Proceedings of the IEEE International Conference on Robotics, pp. 240-247.
- Briot, M. 1979. *The Utilization of an "Artificial Skin" Sensor for the Identification of Solid Objects*. Proceedings of the 9th Symposium on Industrial Robots, pp. 529-548.
- Canny, J.F. 1983. *Finding Edges and Lines in Images*. Technical Report #720, Artificial Intelligence Laboratory, Massachusetts Institute of Technology.
- Clot, J. & Falipou, J. 1978. *Realization D'Otheses Pneumatiques Modulaires: Etude d'un Detecteur de Pressions Plantaires*. Publication LAAS #1852, Centre National de la Recherche Scientifique, Laboratoire d'Automatique et d'Analyse des Systems, Toulouse, France.
- Harmon, L.D. 1982. *Automated Tactile Sensing*. International Journal of Robotics Research, 1(2)3-32.
- Hillis, W.D. 1981. *Active Touch Sensing*. AI Memo 629, Artificial Intelligence Laboratory, Massachusetts Institute of Technology.
- Overton, K.J. 1984. *The Acquisition, Processing, and Use of Tactile Sensor Data in Robot Control*. Technical Report 84-08, Dept. of Computer and Information Science, University of Massachusetts, Amherst MA.
- Raibert, M.H. & Tanner, J.E. 1982. *A VLSI Tactile Array Sensor*. Proceedings of the 12th Symposium on Industrial Robots, pp. 417-425.
- Rebman, J. & Trull, M.W. 1983. *A Robust Tactile Sensor for Robotic Applications*. Proceedings of the International Conference on Computers in Engineering, vol. 2, pp. 109-114.
- Salisbury, J.K. 1984. *Interpretation of Contact Geometries from Force Measurements*. Proceedings of the IEEE International Conference on Robotics, pp. 240-247.
- Wright, 1983. *Technical Description of the Barry Wright Corporation Model 402 Tactile Sensor System*. Barry Wright Corp: 700 Pleasant St, Watertown MA.

Figures

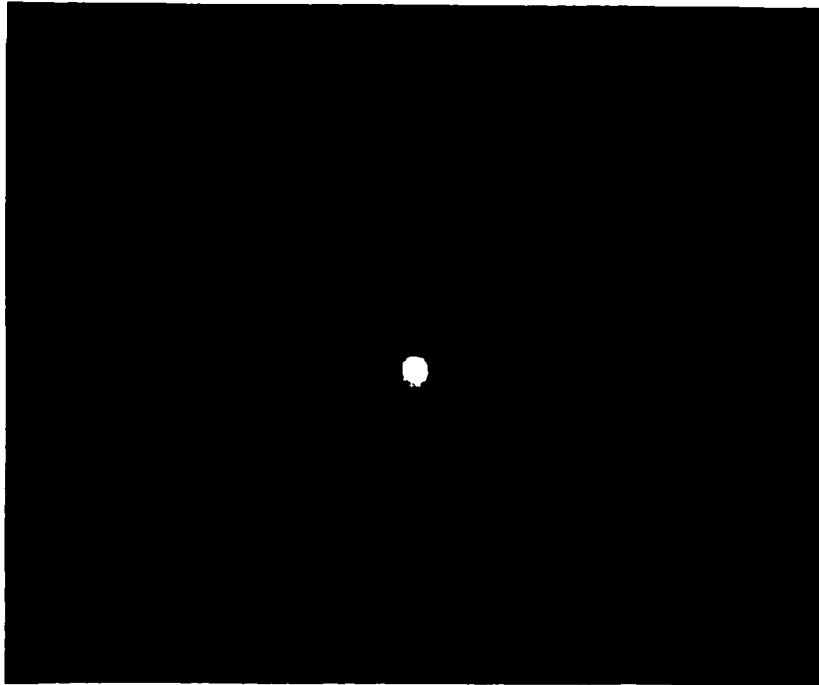


Figure 1
Ball point pen



Figure 2
Line contact, 12 N force

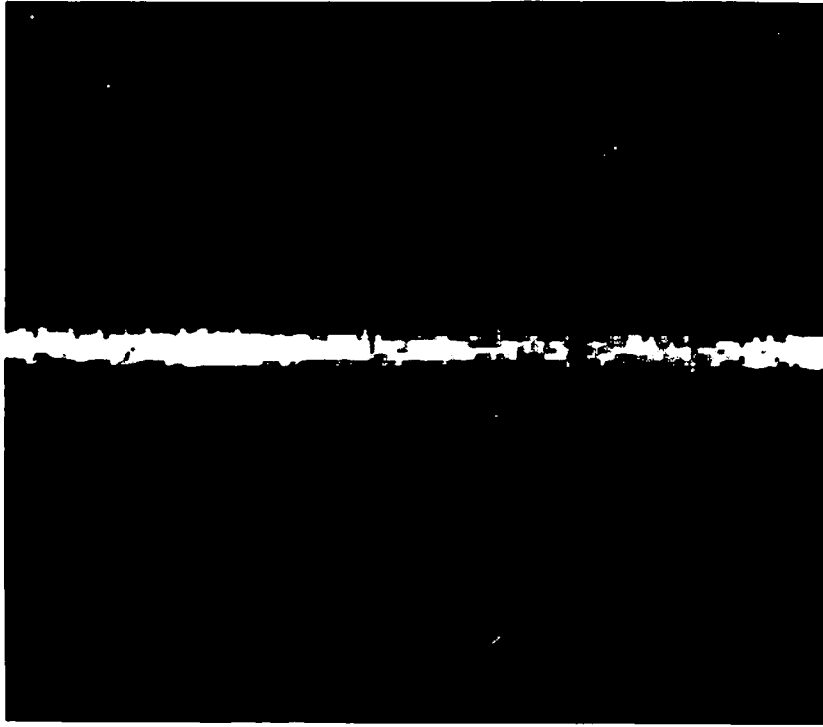


Figure 3A
Line contact, 39 N force

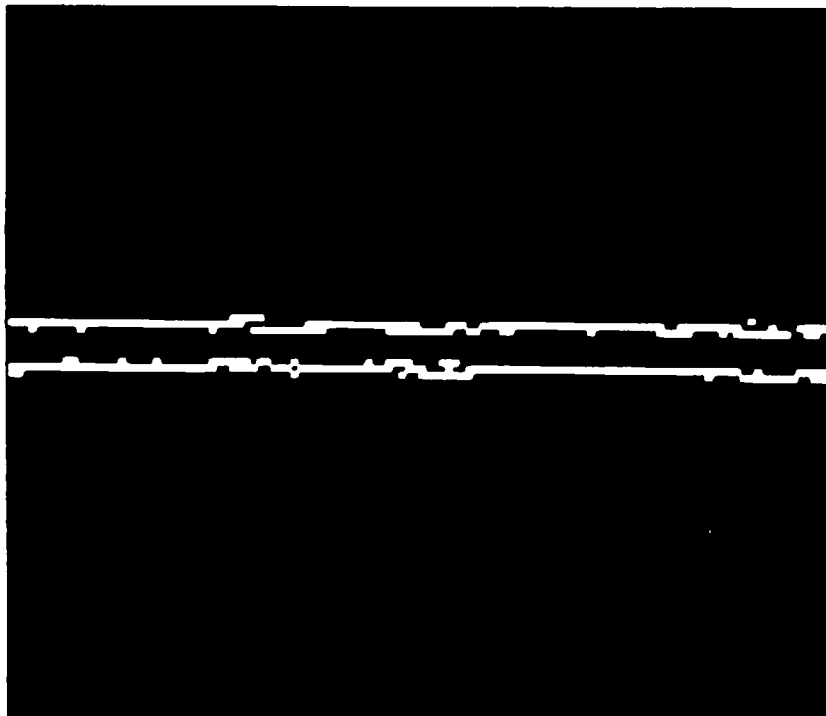


Figure 3B
Edges found from 3A

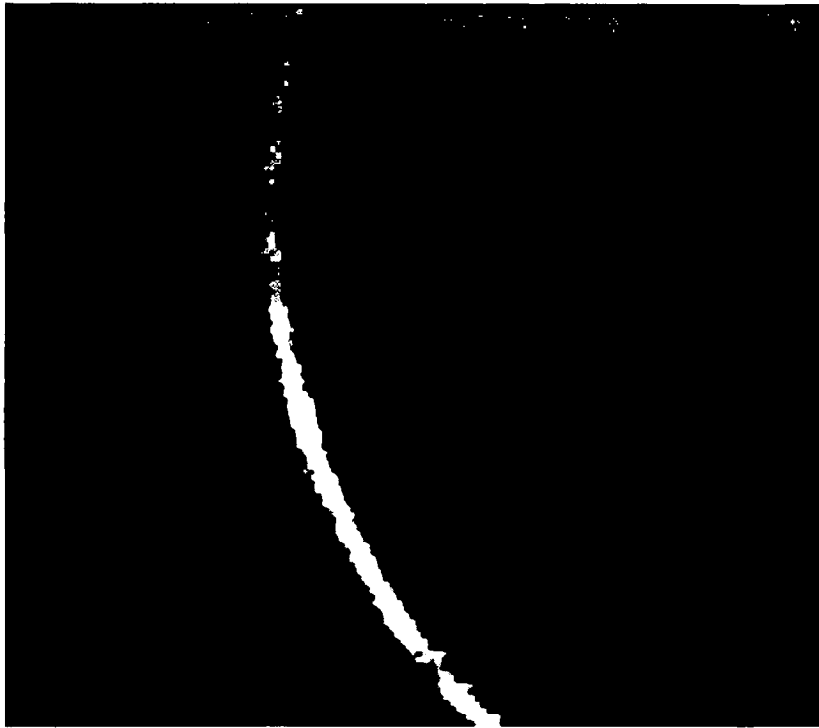


Figure 4A
Top of soft drink can

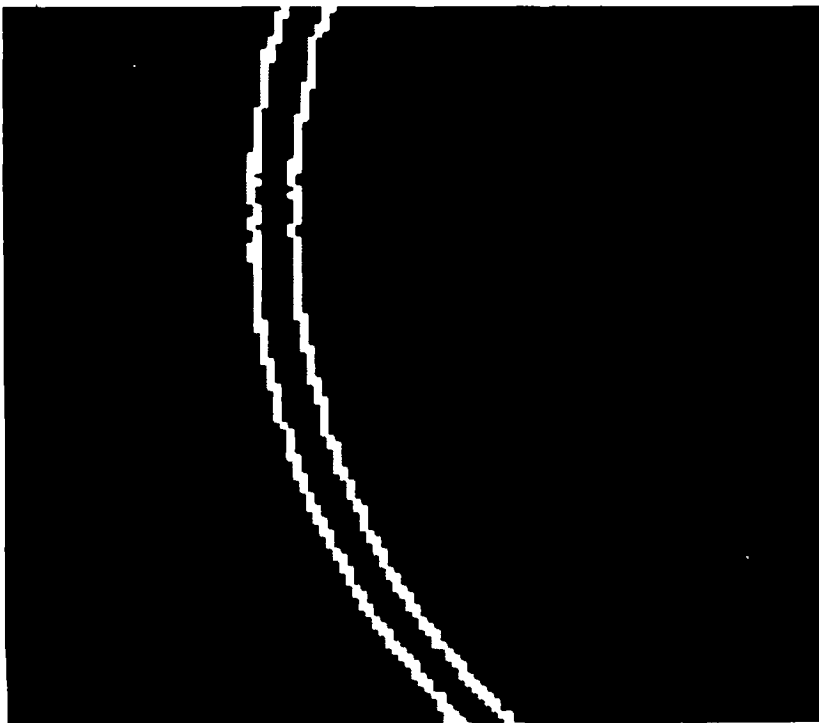


Figure 4B
Edges found from 4A

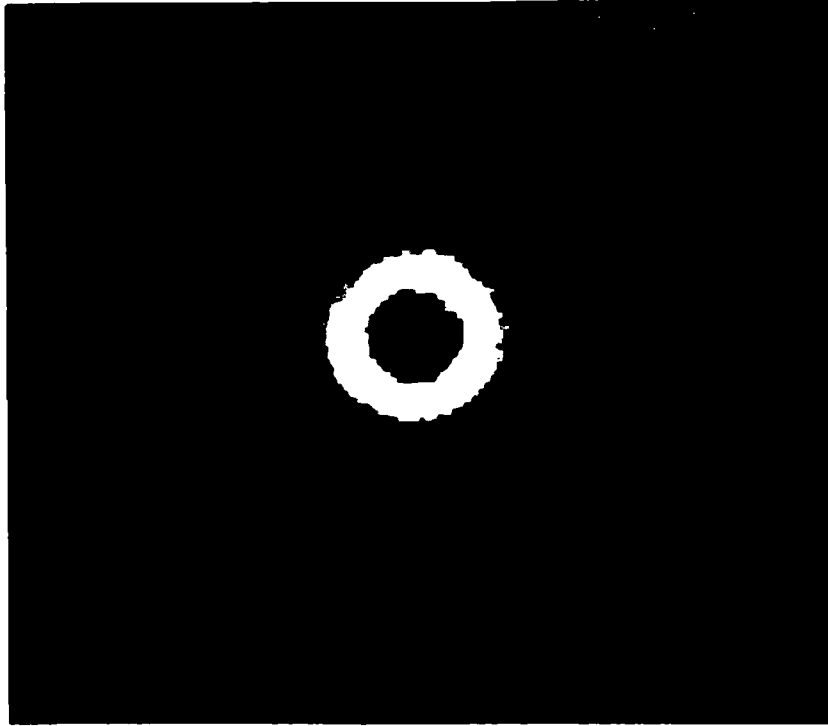


Figure 5A
Washer

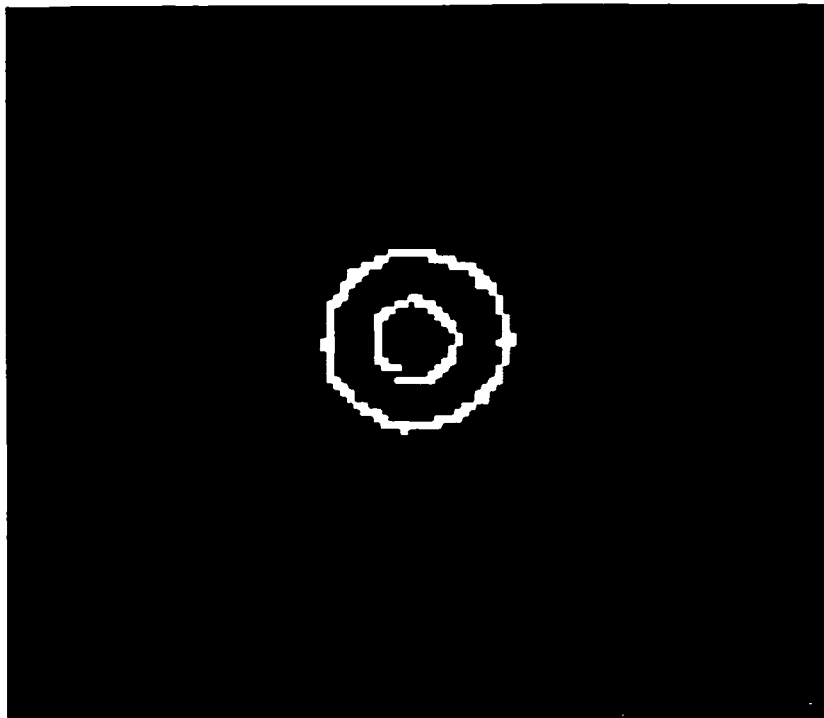


Figure 5B
Edges found from 5A

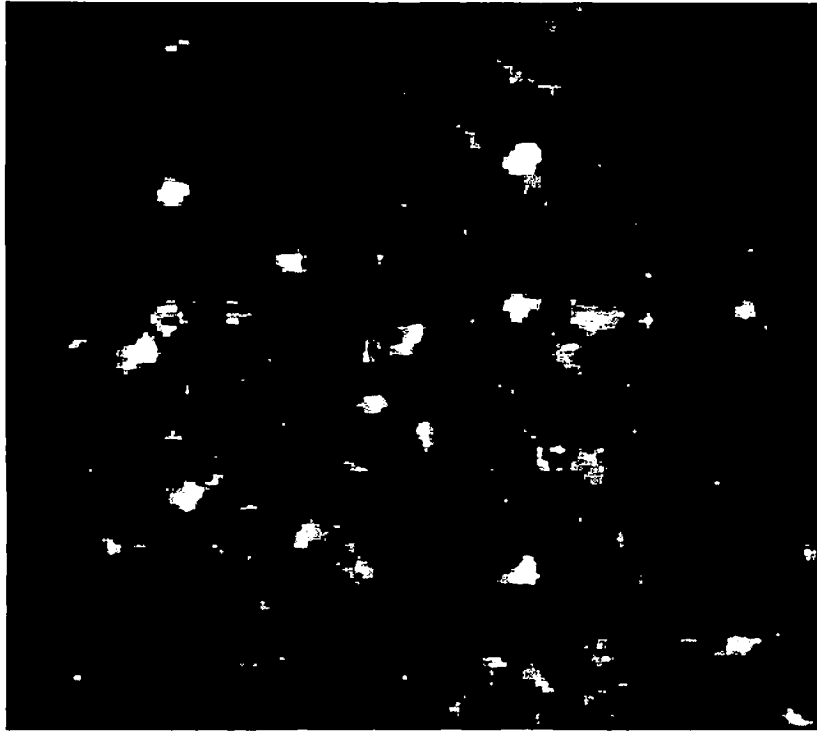


Figure 6
Stiff conductive foam

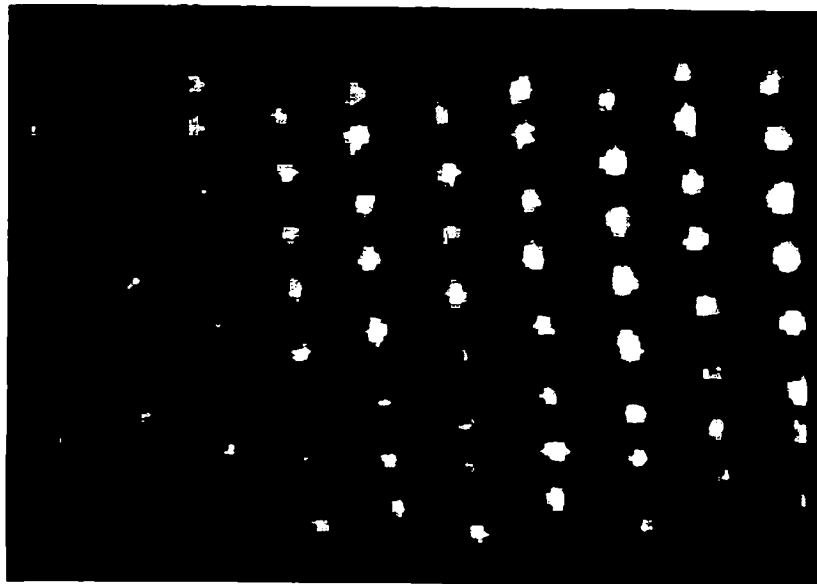


Figure 7
Wood rasp

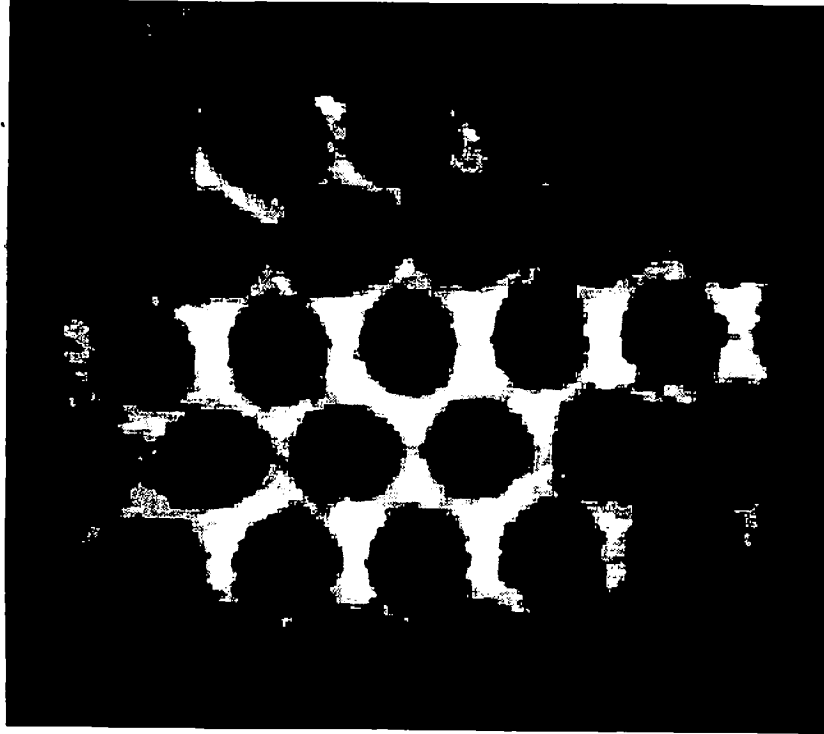


Figure 8
Metal screen, holes = 4 mm dia.

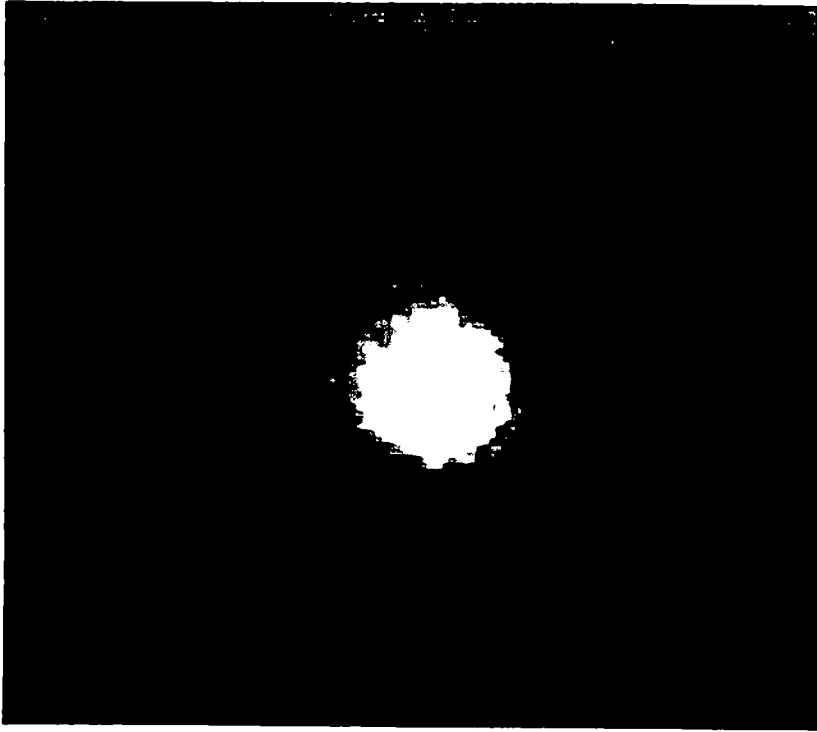


Figure 9A
Racquet ball, 12 N force

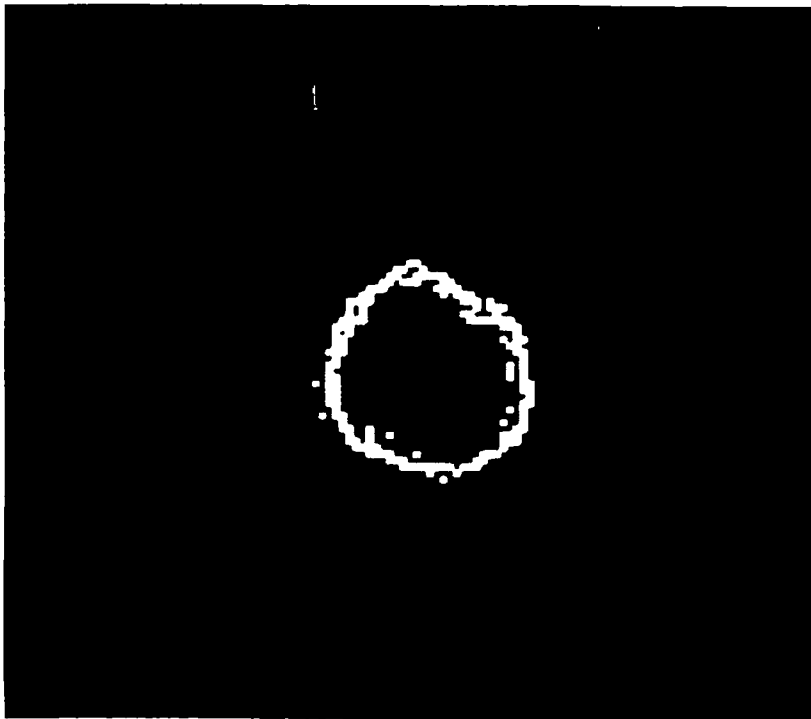


Figure 9B
Edges found from 9A



Figure 10A
Racquet ball, 39 N force

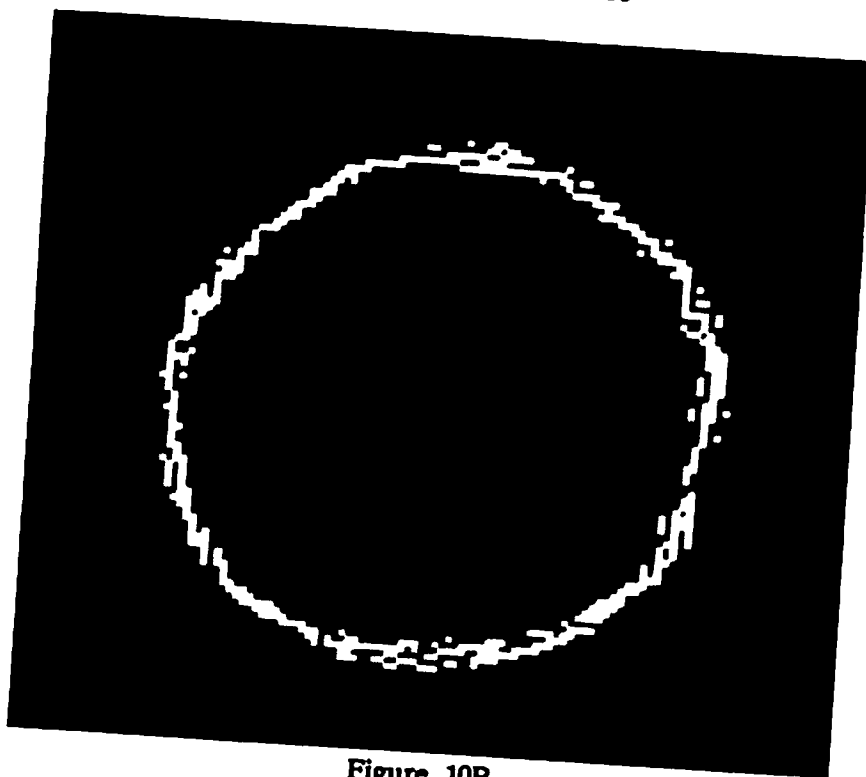


Figure 10B
Edges found from 10A